

# Photophysics of a mono-nuclear tetrahedral silver(I)N<sub>4</sub> core and its copper(I) analog

Shanti G. Patra <sup>a</sup>, Senjuti De <sup>b</sup>, Derek A. Tocher <sup>c</sup> and Dipankar Datta <sup>a,\*</sup>

<sup>a</sup> *Department of Inorganic Chemistry, Indian Association for the Cultivation of Science, Calcutta 700 032, India*

<sup>b</sup> *Dr. Meghnad Saha College, Ranipur, Tilna, WB 733 128, India*

<sup>c</sup> *Department of Chemistry, University College London, 20 Gordon Street, London WC1H 0AJ, UK*

## A B S T R A C T

---

A neutral ligand L is prepared by condensation of benzil dihydrazone and acetone in 1:2 mole ratio and used for the syntheses of [CuL<sub>2</sub>]ClO<sub>4</sub>, [CuL<sub>2</sub>]PF<sub>6</sub>, [AgL<sub>2</sub>]ClO<sub>4</sub> and [AgL<sub>2</sub>]PF<sub>6</sub>. The X-ray crystal structures of L and the two perchlorate salts have been determined. The metal complexes are found to be mononuclear containing tetrahedral N<sub>4</sub> coordination spheres for Cu(I) and Ag(I). Cyclic voltammetrically, the Cu(II/I) and Ag(II/I) potentials are 1.23 and 0.76 V vs NHE respectively in CH<sub>2</sub>Cl<sub>2</sub> at a Pt electrode. The reason for the such a low Ag(II/I) potential is that the silver(I) complex is adsorbed on the electrode surface with a free energy of adsorption of ~ -14.99 kcal mol<sup>-1</sup>. DFT calculations at the BP86/LanL2DZ level show that the HOMO's in [CuL<sub>2</sub>]ClO<sub>4</sub> and [AgL<sub>2</sub>]ClO<sub>4</sub> are both metal based and the LUMO's have no contribution from the metals. Both complexes show weak emissions from the MLCT states upon excitation at 270 nm in ethanol solution at room temperature. Changing the counterion to PF<sub>6</sub><sup>-</sup> leads to higher

quantum yields for these processes. It is consistent with the general observation that  $\text{ClO}_4^-$  being more coordinating than  $\text{PF}_6^-$ , it binds the metals in the MLCT state to form exciplexes leading to a lower  $\phi$  or total quenching. At 77 K in ethanol glass, L,  $[\text{CuL}_2]^+$  and  $[\text{AgL}_2]^+$  show ligand centered (LC) emissions. Thus the MLCT and LC states are thermally equilibrated in the silver(I) and copper(I) complexes. In keeping with this, a mixture of the two processes, MLCT and LC emissions, is observed at room temperature for  $[\text{AgL}_2]\text{ClO}_4$  and  $[\text{CuL}_2]\text{ClO}_4$  when they are incorporated in a rigid polymethyl methacrylate matrix.

---

*Keywords:* X-ray structure, cyclic voltammetry, emission, MLCT, DFT

---

\* Corresponding author. .

*E-mail:* icdd@iacs.res.in

## 1. Introduction

There is significant current interest in the design of transition metal complexes which can emit throughout the visible region [1-5]. Their potential for applications in optoelectronics is enormous [6-13]. In this regard phosphors of Ir(III), Pt(II) and Os(II) are studied most extensively. Some Ir materials have been standard-setting in the field of organic light emitting devices [14,15]. However these metals are very expensive and of limited availability. Consequently, there has been an imperative to find low-cost alternatives and the coinage metals may fill this requirement [12,16-21]. For example, mononuclear Cu(I) complexes of the type  $[\text{Cu}(\text{N-N})(\text{P-P})]^+$  where N-N is a 1,4-diimine like 1,10-phenanthroline (phen) and P-P a bidentate phosphine, are found to have emission properties like those of the best Ir(III) complexes [19,22,23]. Here we are concerned with the basics of the photophysics of mononuclear tetrahedral homoleptic Cu(I) and Ag(I) complexes of a 1,4-diazine (L; Chart 1). While examples of mononuclear

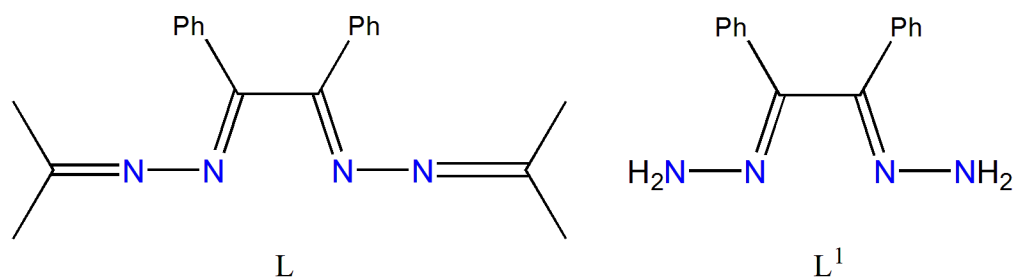


**Chart 1** Ligands involved in the present work

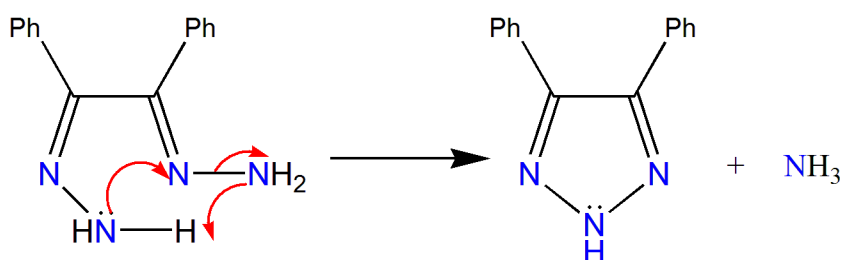
$\text{Cu}^{\text{I}}\text{N}_4$  core are abundant, similar complexes of Ag(I) are rare. As such, photophysics of Ag(I) complexes with tetrahedral coordination geometry similar to their Cu(I) analogs has been seldom studied, possibly because of their light sensitivity and limited luminescent properties [18,21,24]. Thus of the numerous reports on emissive silver(I) complexes to date most involve multinuclear compounds usually having an Ag(I)...Ag(I) bond [11,25,26].

## 2. Results and discussion

Copper(I) complexes of N-donor ligands are usually air sensitive mainly because of the low potential for the Cu(II/I) couple. This air sensitivity of the copper(I) complexes

has been effectively exploited by many workers to generate interesting copper(I)-dioxygen chemistry [27-29]. Generation of an air stable  $\text{CuN}_4^+$  core requires a ligand that can destabilize the corresponding copper(II) species [30,31]. One way of achieving this is to impose a tetrahedral coordination geometry on the copper(II) species, which requires carefully designed ligands. We believe benzil dihydrazone ( $\text{L}^1$ ) to be a potential candidate in this regard, as it has a twisted conformation with the torsion angle  $\text{N}=\text{C}-\text{C}=\text{N}$  of  $\sim 70^\circ$  in the solid state [32].

Reaction of  $\text{L}^1$  with  $\text{Cu}(\text{MeCN})_4\text{ClO}_4$  in dry methanol under  $\text{N}_2$  in a 2:1 molar ratio at room temperature yields an air stable yellow copper(I) complex of the formulation  $[\text{Cu}(\text{DPT})]\text{ClO}_4$  ( $\text{DPT} = 4,5\text{-diphenyl-}2H\text{-}[1,2,3]$  triazole). A tentative mechanism for the metal-assisted conversion of  $\text{L}^1$  to  $\text{DPT}$  is proposed in Scheme 1 [33]. Our attempts to isolate the organic moiety in  $[\text{Cu}(\text{DPT})]\text{ClO}_4$  in the free state by treating the complex with ammonia have resulted in the isolation of  $\text{L}^1$  only.



**Scheme 1**

Realizing that the free  $\text{NH}_2$  groups of  $\text{L}^1$  are problematic, we have capped them by reaction with acetone, i.e. we have prepared the 1:2 acetone condensate ( $\text{L}$ ) of  $\text{L}^1$  which is characterised by X-ray diffraction (Fig. 1).  $\text{L}$  is observed to adopt a staggered conformation about the  $\text{C}1-\text{C}11$  bond ( $\text{C}12-\text{C}11-\text{C}1-\text{C}2 = 85.0^\circ$ ,  $\text{N}1-\text{C}1-\text{C}11-\text{N}3 = 90.6^\circ$ ) in order to minimize the steric interactions between the phenyl groups. The  $\text{C}=\text{N}$  bond lengths are all closely similar (1.263(3)-1.279(3) Å) and the  $\text{N}-\text{N}$  bonds (1.401(3) and 1.403(3) Å) are somewhat shorter than the conventional single bond length (1.46 Å) between a pair of nitrogen atoms due to conjugation. Selected crystal data for  $\text{L}$  are given in Table 1. Its  $^1\text{H}$  NMR spectrum is shown in Fig. S1 as supplementary material.

The reaction of  $\text{L}$  with copper(II)acetate monohydrate in methanol in 2:1 molar ratio and subsequent addition of an excess of  $\text{NaClO}_4 \cdot \text{H}_2\text{O}$  gave yellow crystals of the

copper(I) complex  $[\text{CuL}_2]\text{ClO}_4$ . The same compound is obtained from the reaction of L with  $[\text{Cu}(\text{MeCN})_4]\text{ClO}_4$  in a 2:1 molar ratio in methanol under  $\text{N}_2$  atmosphere. The complex crystallizes in the monoclinic space group  $\text{C}2/c$  with two cations, each located on a two fold axis (therefore only half of each cation is crystallographically unique), and one ordered perchlorate anion in the asymmetric unit. The two cations are essentially identical in all significant aspects of their geometry and one of them is shown in Fig. 2. Selected crystal data for  $[\text{CuL}_2]\text{ClO}_4$  are given in Table 1. The copper is ligated by two bidentate ligands and the geometry about Cu1 is distorted tetrahedral with the four independent angles subtended by the ligating atoms being  $95.75(9)$ ,  $96.81(9)$ ,  $105.34(7)$  and  $128.76(7)^\circ$ . The two smaller values are due to the bidentate bite of the two seven-membered chelates. Earlier we have seen that when the phenyl rings of L are replaced by methyl groups, the resulting ligand L' binds Ru(II) in  $[\text{Ru}(\text{bpy})_2\text{L}']^{2+}$  (bpy = 2,2'-bipyridine) in a fashion such that a five-membered chelate ring is generated with smaller bite angle,  $\sim 76^\circ$  [34]. Chelation affects the conformation adopted by L in  $[\text{CuL}_2]^+$  such that the torsion angles noted in the free ligand are reduced by about  $20^\circ$  ( $\text{C}5\text{-C}4\text{-C}4\text{A-C}4 = 66.0$ ,  $\text{N}2\text{-C}4\text{-C}4\text{A-N}2\text{A} = 77.7$ ,  $\text{C}15\text{-C}14\text{-C}14\text{A-C}15\text{A} = 71.8$ ,  $\text{N}4\text{-C}14\text{-C}14\text{A-N}4\text{A} = 76.3^\circ$ ). The C=N and N-N bond lengths in the coordinated ligands are not significantly different from those observed for the free ligand. The two Cu-N distances in  $[\text{CuL}_2]^+$  are closely similar ( $2.049(2)$  and  $2.055(2)$  Å). The two  $\text{CuN}_2$  planes intersect each other at  $\sim 72^\circ$ . Though the unit cell of  $[\text{CuL}_2]\text{ClO}_4$  contains two independent cations, its solution  $^1\text{H}$  NMR spectrum in  $\text{CDCl}_3$  (Fig. S2; supplementary material) shows that the cation has  $\text{C}_2$  symmetry in solution. The methyl signals of the chelated L are deshielded slightly compared to those of the free L. The aromatic protons appear as better resolved in the  $^1\text{H}$  NMR spectrum of the copper(I) complex than in free L. In free L, meta and para protons appear at the same chemical shift.

Reaction of  $\text{Ag}(\text{ClO}_4) \cdot x\text{H}_2\text{O}$  with L at room temperature in methanol in a 1:2 molar ratio yields white crystals of  $[\text{AgL}_2]\text{ClO}_4$ . The silver complex crystallises in the chiral orthorhombic space group  $\text{P}2_12_12_1$  with one cation and one disordered perchlorate anion in the asymmetric unit (Fig. 3). Selected crystal data are given in Table 1. The four Ag-N bonds fall in a relatively narrow range ( $2.301(2)$ - $2.324(2)$  Å) and are substantially longer than those observed in the copper complex, however, the difference closely

matches that between the reported ionic radii of  $\text{Cu}^+$  and  $\text{Ag}^+$ . The distortions from ideal tetrahedral geometry are larger than those observed in the isostructural copper complex, with the six tetrahedral angles ranging from  $88.86(6)$  to  $129.30(7)^\circ$ . Nevertheless, it is worth noting that the torsions observed about the C-C bond in the two coordinated ligands are on average larger for the silver complex,  $75.1^\circ$ , than they were for the copper complex,  $72.9^\circ$ , presumably as a consequence of the longer metal-ligand bonds in the former. The conformation of the ligand in the silver complex is closer to that of the free ligand than was the case in the copper complex. As expected the calculated average Ag-N bond length ( $2.32 \text{ \AA}$ ) is longer than that of the corresponding copper complex ( $2.05 \text{ \AA}$ ). The chelate rings are again seven-membered. The angles of intersection of the two  $\text{AgN}_2$  planes in  $[\text{Ag}(\text{bpy})_2]\text{ClO}_4$  and  $[\text{Ag}(\text{phen})_2]\text{ClO}_4$  are  $39^\circ$  and  $31^\circ$  respectively [35], while that in  $[\text{Ag}(\text{bpy})_2]\text{ClO}_4$  is  $\sim 75^\circ$ . For an ideal tetrahedron, this angle should be  $90^\circ$ . So in our case the  $\text{Ag}^1\text{N}_4$  core is much more tetrahedron like than in its bpy or phen analog. Examples of mononuclear complexes containing the  $\text{AgN}_4$  core are rare and most reported examples are square planar [36,37], which is a high energy geometry for  $d^{10}$  Ag(I) [38]. The  $^1\text{H}$  NMR spectrum of  $[\text{AgL}_2]\text{ClO}_4$  (Fig. 4) reveals that the cation also has a  $\text{C}_2$  axis in the solution like  $[\text{CuL}_2]^+$ . Upon coordination to Ag(I), the methyl signals of the free L are shifted downfield as in  $[\text{CuL}_2]\text{ClO}_4$  (see Figs. S1 and S2 in the supplementary material). The NMR spectra match well with the theoretical ones derived by the GIAO method as implemented in GAUSSIAN09 (see Table S1 in the supplementary material).

An interesting result of our single point DFT calculations at the BP86/LanL2DZ level, on the crystallographic geometries (after adjusting all the C-H bond lengths to  $1.09 \text{ \AA}$ ) of L,  $[\text{CuL}_2]\text{ClO}_4$  and  $[\text{AgL}_2]\text{ClO}_4$  indicate that the conformation of the chelated L is more stable than that of the free ligand by  $3.50 \text{ kcal mol}^{-1}$  in the copper(I) complex and by  $3.67 \text{ kcal mol}^{-1}$  in the silver(I) analog, i.e. the free ligand is more strained than the coordinated one. That it is due to the crystal packing effects in the solid state, is evident from our single point DFT calculations on L,  $[\text{CuL}_2]\text{ClO}_4$  and  $[\text{AgL}_2]\text{ClO}_4$  at their optimized geometries in the gas phase where the chelated L is found to be less stable than the free L by  $3\text{-}4 \text{ kcal mol}^{-1}$ .

The electrochemical behaviour of  $[\text{CuL}_2]\text{ClO}_4$  and  $[\text{AgL}_2]\text{ClO}_4$  have been studied by cyclic voltammetry at a Pt electrode in purified  $\text{CH}_2\text{Cl}_2$ . The copper(I) complex displays a quasi-reversible Cu(II/I) couple on the positive side of normal hydrogen electrode (NHE) (Fig. 5) with a half-wave potential ( $E_{1/2}$ ) of 1.23 V. The highest potential reported so far for the Cu(II/I) couple of a complex with a  $\text{Cu}^{\text{I}}\text{N}_4$  core is 1.79 vs NHE [39]. The Cu(II/I) potential in a  $\text{Cu}^{\text{I}}\text{N}_4$  chromophore is believed to increase with (1) the  $\pi$ -acidity of the ligand(s) (which preferentially stabilizes the oxidation state I of copper) and (2) the extent of tetrahedral distortion occurring in the corresponding  $\text{Cu}^{\text{II}}\text{N}_4$  core (which preferentially destabilizes  $d^9$  Cu(II) whose natural tendency is to adopt square planar geometry so that it can maximise crystal field stabilization energy) [40]. Both factors seem to be operating here. There is extensive conjugation in the ligand L to preferentially stabilize Cu(I). Further, the steric effects of the methyl groups in L seem to force the copper(II) center in the electrogenerated species to adopt a distorted tetrahedral geometry. The Cu(II/I) potential is so high that the corresponding copper(II) species can oxidize water. This is consistent with the observation that when  $\text{Cu}(\text{acetate})_2 \cdot \text{H}_2\text{O}$  is used in the synthesis, we obtain the copper(I) complex only.

On the other hand, under identical experimental conditions as those used for the copper(I) complex, the  $E_{1/2}$  of the Ag(II/I) couple in the silver(I) complex is comparatively low, 0.76 V vs NHE (Fig. 6). The formal potential of the Ag(II/I) couple in 1-4 mol  $\text{dm}^{-3}$   $\text{HNO}_3$  is 1.93 V vs NHE [41]. N-donor ligands stabilize Ag(II) much through coordination. As a result, the Ag(II/I) potential decreases. For example, this potential in  $[\text{Ag}(\text{bpy})_2]^+$  is 1.30 V vs NHE in propylene carbonate [42]. In our complex, the  $\text{Ag}^{\text{I}}\text{N}_4$  is more tetrahedral than in its bpy counterpart. Since Ag(II) is  $d^9$  like Cu(II), the factors which raise the Cu(II/I) potential, also increase the Ag(II/I) potential. A tetrahedral geometry is destabilizing for Ag(II). Thus the Ag(II/I) potential in our complex is expected to be more than 1.30 V vs NHE. We have calculated the relative stability (free energy wise; Table S2) of Cu(I) w.r.t. Cu(II) and vis-à-vis Ag(I) w.r.t. Ag(II) at the BP86/LanL2DZ level at the optimised geometries) which are respectively -200.35 and -204.51 kcal  $\text{mol}^{-1}$ . They indicate that in our complexes Ag(II/I) potential should be higher than the Cu(II/I) potential by 0.18 V. Thus the Ag(II/I) couple should have an  $E_{1/2}$  of  $1.23 + 0.18 = 1.41$  V vs NHE. This value matches with our expectation

that the Ag(II/I) couple should have a potential higher than that in  $[\text{Ag}(\text{bpy})_2]^+$ . In reality, it is 0.76 V vs NHE with a difference of 0.65 V which is -14.99 kcal mol<sup>-1</sup>. We attribute this much energy to the free energy change for adsorption of the silver species on to the electrode [43,44]. In keeping with this, the voltammogram obtained in Fig. 6 is indeed characteristic of adsorption. The anodic peak current  $i_{\text{pa}}$  varies linearly with scan rate (Fig. 6). Usually, when the magnitude of the free energy is more than 5 kcal mol<sup>-1</sup>, it is considered to be chemisorption.

We have examined the photophysical behaviour of the ligand L and its two complexes  $[\text{CuL}_2]\text{ClO}_4$  and  $[\text{AgL}_2]\text{ClO}_4$ . In the electronic spectra in  $\text{CH}_2\text{Cl}_2$ , all the three compounds display a strong absorption around 270 nm (Fig. 7). The extinction coefficient of this band in L is  $\sim 33,000 \text{ dm}^3 \text{ mol}^{-1} \text{ cm}^{-1}$  and those in the complexes are 50,000 – 60,000  $\text{ dm}^3 \text{ mol}^{-1} \text{ cm}^{-1}$ . Upon excitation at 270 nm in ethanol, L is found to be virtually non-emissive (Fig. 8) but the two perchlorate complexes produce weak emissions (ethanol is chosen as it forms a glass of good quality at 77 K). The emission maxima  $\lambda_{\text{em}}$  for  $[\text{CuL}_2]\text{ClO}_4$  is 400 nm and that for the silver analog 387 nm (Fig. 8). The quantum yields  $\phi$  have been determined relative to tryptophan in water ( $\lambda_{\text{ex}}$ , 275 nm;  $\lambda_{\text{em}}$ , 375 nm;  $\phi$ , 0.14) [45] correcting for changes in the refractive index, Table 2. The  $\phi$  for  $[\text{CuL}_2]\text{ClO}_4$  is slightly greater than that for  $[\text{AgL}_2]\text{ClO}_4$ .

The first observation of photoluminescence from a  $\text{Cu}^{\text{I}}\text{N}_4$  chromophore was made by Buckner and McMillin in 1978 in ethanol glass at 77 K [46]. The relevant copper(I) species was  $[\text{Cu}(\text{dmp})_2]^+$  where dmp is 2,9-dimethyl-phen. Subsequently, McMillin and co-workers reported emission from  $[\text{Cu}(\text{dmp})_2]\text{BF}_4$  in  $\text{CH}_2\text{Cl}_2$  solution at room temperature [47]. This report triggered a flurry of activity in the photophysical and photochemical studies on Cu(I) complexes of N-donor ligands [16,48,49]. This culminated in the discovery of highly luminescent mixed ligand complexes of the type  $[\text{Cu}(\text{N-N})(\text{P-P})]^+$  where P-P is a bidentate phosphine and N-N a phen-like ligand(vide supra). In our  $[\text{CuL}_2]\text{ClO}_4$ , the  $\phi$  in ethanol at room temperature is  $1 \times 10^{-3}$  (Table 2). The emission in our complex is somewhat stronger than that in  $[\text{Cu}(\text{dmp})_2]\text{BF}_4$  as  $\phi$  observed for the latter in  $\text{CH}_2\text{Cl}_2$  is  $2\text{-}4 \times 10^{-4}$  [47,50]. It is now well understood from ultrafast spectroscopy [49,51] that the emission in a  $\text{Cu}^{\text{I}}\text{N}_4$  chromophore originates from a metal-to-ligand charge transfer (MLCT) state. In the MLCT state Cu(I) is converted into Cu(II).

Due to the different structural requirements of the two oxidation states of copper, it is reasonable to assume that a flattening of the metal geometry in the MLCT state leads to quenching. So, for emission from a  $\text{Cu}^{\text{I}}\text{N}_4$  core to occur the geometrical change at the metal in going from oxidation state I to II should be a minimum. Thus while  $[\text{Cu}(\text{dmp})_2]^+$  is photoluminescent,  $[\text{Cu}(\text{phen})_2]^+$  is not, even at 77 K, due to the severe flattening of the Cu(II) species generated in the excited state where steric clashes are totally absent [48,49]. To ascertain that the observed emission for  $[\text{CuL}_2]\text{ClO}_4$  is from MLCT state(s), we have evaluated its HOMO and LUMO by BP86/LanL2DZ calculations. From the pictorial representations in Table 3, we find that the HOMO is metal based while the LUMO has no contribution from the metal.

Our silver(I) complex  $[\text{AgL}_2]\text{ClO}_4$  shows weaker emission than its copper(I) analog (Fig. 8; Table 2). No MLCT emission has ever been observed for a mononuclear Ag(I) complex [12,16,52]. As one moves down the group from Cu(I) to Ag(I), the effective nuclear charge increases leading to a greater net electron-nucleus attraction. Consequently, the d orbitals of Ag(I) become lower in energy rendering metal oxidation more difficult. As a result, the Ag(I) ion becomes more resistant to oxidation than Cu(I), and unlike in the mononuclear Cu(I) emissive compounds, the HOMO of mononuclear Ag(I) compounds often contains no silver contribution and the luminescent Ag(I) complexes show emission usually due to a ligand-centered  $\pi\pi^*$  transition [12,16,52]. From the BP86/LanL2DZ calculations, we find that the HOMO of  $[\text{AgL}_2]^+$  has a significant component from the metal and the LUMO is totally localized on the ligands (Table 3). It is known from extensive photophysical studies on  $\text{Cu}^{\text{I}}\text{N}_4$  that coordinating solvents or anions quench the emission. This is due to the fact that as the metal becomes Cu(II),  $d^9$  it tries to expand its coordination sphere in the excited state and binds at least one additional coordinating species forming an exciplex which causes a decrease in, or quenching of, the emission. The order of the coordinating ability of some common anions are as follows:  $\text{BPh}_4^- < \text{PF}_6^- < \text{BF}_4^- < \text{ClO}_4^- < \text{NO}_3^-$  [53]. Hence  $\text{ClO}_4^-$  is a more powerful quencher than  $\text{PF}_6^-$ , i.e. emission of the  $\text{PF}_6^-$  salt of  $[\text{CuL}_2]^+$  should be stronger than that of the  $\text{ClO}_4^-$  salt. This is indeed found to be true in our Cu(I) complex of L. The  $\phi$  of  $[\text{CuL}_2]\text{PF}_6$  is twice than that of  $[\text{CuL}_2]\text{ClO}_4$  in ethanol at room temperature (Fig. 8; Table 2). Since Ag(II) is also  $d^9$  the coordination behaviour of the metals in the excited state is

expected to be similar. Accordingly,  $[\text{AgL}_2]\text{PF}_6$  is found to be a much stronger emitter than  $[\text{AgL}_2]\text{ClO}_4$  (Fig. 8; Table 2); replacement of the  $\text{ClO}_4^-$  by  $\text{PF}_6^-$  brings about five fold increase in the  $\phi$  of the emission of the cation  $[\text{AgL}_2]^+$ . This in a way proves that the emission observed in  $[\text{AgL}_2]\text{ClO}_4$  in ethanol at room temperature is from an MLCT excited state. Interestingly, though no one has ever observed an MLCT transition for an  $\text{Ag}^{\text{I}}\text{N}_4$  chromophore, it is invoked to explain the generally observed near square planar geometry of an  $\text{Ag}^{\text{I}}\text{N}_4$  core. It is argued that the admixture of the MLCT configuration, (e.g.  $\text{Ag}^+(\text{bpy}) \rightarrow \text{Ag}^{2+}(\text{bpy}^-)$ ) into the ground state wave function leads to flattening of an  $\text{Ag}^{\text{I}}\text{N}_4$  core [54,55].

We have recorded the emission spectra of L,  $[\text{CuL}_2]\text{ClO}_4$  and  $[\text{AgL}_2]\text{ClO}_4$  in an ethanol glass at 77 K. These spectra are highly structured with emission maxima at 428 nm (Fig. 9). We assign these bands to ligand-centered (LC) emission, as LC emission maxima do not change with the metal in the complex, though  $\phi$  can differ [56,57]. This means that LC and MLCT states are thermally equilibrated in our metal complexes, with the LC state being the lowest excited state at low temperature. This observation is supported by the emissions of L,  $[\text{CuL}_2]\text{ClO}_4$  and  $[\text{AgL}_2]\text{ClO}_4$  in a polymethyl methacrylate (PMMA) film (Fig. 10) where we can see a weak emission from L and much stronger emissions from its metal complexes. The  $\lambda_{\text{em}}$  for L is 485 nm and this emission is present in the spectra of the metal complexes as a shoulder. The  $\lambda_{\text{em}}$  for  $[\text{CuL}_2]\text{ClO}_4$  is 452 nm and that for  $[\text{AgL}_2]\text{ClO}_4$  395 nm. Thus an unequal admixture of LC and MLCT emissions is observed for the perchlorate complexes in the rigid PMMA matrix.

### 3. Concluding remarks

Here we have characterized an unusual mono-nuclear tetrahedral  $\text{Ag}^{\text{I}}\text{N}_4$  core. The ligand L used is a simple bidentate N,N-donor, although the donor atoms are relatively uncommon azino nitrogen atoms. Our structural studies indicate that we have been able to house an  $\text{Ag}(\text{I})$  center in a tetrahedral  $\text{N}_4$  environment. The results have been remarkable. The HOMO of  $[\text{AgL}_2]^+$  is metal based, which is not an usual situation in  $\text{Ag}(\text{I})$  complexes of N-donor ligands. As expected, the HOMO in  $[\text{CuL}_2]^+$  is metal based. Both the complexes of silver(I) and copper(I) exhibit photoluminescence from an MLCT

state in ethanol at room temperature. That the emission is from an MLCT state is clear from the fact that the quantum yield  $\phi$  for  $[\text{AgL}_2]\text{PF}_6$  is much higher than for  $[\text{AgL}_2]\text{ClO}_4$ . From extensive studies on the photophysics of  $\text{Cu}^{\text{I}}\text{N}_4$ , it is known that  $\text{ClO}_4^-$  is much more coordinating than  $\text{PF}_6^-$ , it forms an exciplex by binding to the metal in the excited state resulting in a decrease in, or quenching of, the emission. However, L,  $[\text{CuL}_2]^+$  and  $[\text{AgL}_2]^+$  show LC emission in ethanol glass at 77 K. Admixtures of MLCT and LC emissions are observed at room temperature in the photoluminescence of  $[\text{AgL}_2]\text{ClO}_4$  and  $[\text{CuL}_2]\text{ClO}_4$  in a rigid PMMA matrix.

## 4. Computational

All the DFT calculations were carried out by using GAUSSIAN09 package [58]. Inputs for the L,  $[\text{CuL}_2]^+$  and  $[\text{AgL}_2]^+$  were generated from the respective crystal structures. Functional used here is BP86 [59-61] along with the LanL2DZ [62,63] basis set. To check the conformational stability of the ligand, single point energy calculations of the free ligand and in its metal complexes were carried out at the X-ray crystallographic geometry. To calculate the relative stability of the metal complexes in the +1 and +2 oxidation state geometry optimisation of the metal complexes in both the oxidation states were carried out. To confirm the identification of true minima, frequency calculations were performed. Pictorial representations of the various m.o.s were generated from the respective .chk file by GaussView 5.0. Absolute shielding for all hydrogen atoms in the optimized structures of L,  $[\text{CuL}_2]^+$  and  $[\text{AgL}_2]^+$  were calculated using the GIAO approximation at the HF/6-31G(d) level (LanL2DZ basis set is used for the Ag atom) of theory. Theoretical chemical shifts were calculated using the direct subtraction of the calculated absolute shielding of TMS ( $\delta_{\text{TMS}}$ ) [64].

## 5. Experimental

### 5.1 Materials and physical measurements

$\text{NaClO}_4 \cdot x\text{H}_2\text{O}$ ,  $\text{AgClO}_4 \cdot x\text{H}_2\text{O}$ ,  $\text{NH}_4\text{PF}_6$ ,  $\text{AgNO}_3$ , TBAP and PMMA powder (average  $M \sim 120,000$ ) were purchased from Sigma-Aldrich and were used as received.  $[\text{Cu}(\text{MeCN})_4]\text{ClO}_4$  was prepared by a literature method [65] and  $\text{L}^1$  by a procedure

reported elsewhere [32] by us. Microanalyses were performed by a Perkin-Elmer 2400II CHNS analyser. Molar conductance was measured in methanol by a Sytronics (India) conductivity meter (model 306). FTIR spectra (KBr) were recorded on a Shimadzu FTIR-8400S spectrometer and UV-Vis spectra on a Perkin Elmer Lambda 950 spectrophotometer. 500 MHz NMR spectra were recorded on a Bruker Avance III 500 spectrometer in  $\text{CDCl}_3$  unless otherwise specified and ESI mass spectra (in  $\text{CH}_3\text{CN}$ ) on a Waters Qtof Micro YA263 spectrometer. Emission spectra were recorded by a Perkin Elmer LS55 spectrometer (Light source: a xenon discharge lamp, equivalent to 20 kW for 8  $\mu\text{s}$  duration. Pulse width at half height:  $<10 \mu\text{s}$ . Sample detector: a gated photomultiplier with a modified S5 response. Reference detector: a photodiode. Monochromators: Monk-Gillieson type) in ethanol. Cyclic voltammetry was performed with a conventional three-electrode system at room temperature using a CHI600E electrochemical analyzer. An Ag/AgCl electrode was used as the reference. A Pt electrode was used as the working one. All photophysical and other measurements were done with single crystals which are readily obtained from methanol solutions by slow aerial evaporation.

### 5.2 Synthesis of $[\text{Cu}(\text{DPT})]\text{ClO}_4$

$\text{L}^1$  (0.238 g, 0.1 mmol) was added to dry methanol (10 ml) and stirred under  $\text{N}_2$  for 10 minutes. To the ligand solution  $[\text{Cu}(\text{MeCN})_4]\text{ClO}_4$  (0.164 g, 0.5 mmol) was added and stirred. An orange red colour solution was formed immediately after the addition of metal salt. The reaction mixture was then further stirred for 30 minutes. Then diethyl ether (25 ml) was added with stirring. The yellow precipitate formed was filtered out and dried in vacuo over fused  $\text{CaCl}_2$ . Yield: 0.12 g (62 %). Anal. Calc. for  $\text{C}_{14}\text{H}_{11}\text{N}_3\text{CuClO}_4$ : C, 43.76; H, 2.89; N, 10.94. Found: C, 43.81; H, 2.83; N, 10.78%. FTIR  $\nu/\text{cm}^{-1}$ : 3579m, 3508m, 2926w, 1602w, 1144s, 1110s, 1084s, 758w, 681w.  $^1\text{H}$  NMR ( $\text{CD}_2\text{Cl}_2$ )  $\delta/\text{ppm}$ : 7.09-7.75 (m, 10H, aromatic protons).  $\Lambda_{\text{M}}/\text{mho cm}^2 \text{mol}^{-1}$ : 81 (1:1 electrolyte).

### 5.3 Synthesis of Ligand $L$

$\text{L}^1$  (0.48 g, 2 mmol) was added to acetone (30 ml) and refluxed for 9 h. The resulting clear yellow solution was then left to evaporate in air. When the volume

reduced to ca. 5 ml, the white crystalline compound with a tinge of yellow appeared was filtered, washed with cold methanol (2 ml) and then dried in air. Yield, 0.625 g (98%). Anal. calcd for  $C_{20}H_{22}N_4$ : C, 75.44; H, 6.96; N, 17.60. Found: C, 75.73; H, 6.90; N, 17.46 %. FTIR  $\nu/cm^{-1}$ : 3433br, 2916w, 1629vs, 1491m, 1444s, 1429s, 1360s, 1242s, 1178w, 1074w, 1026w, 930w, 750s, 692vs, 649m, 574m.  $^1H$  NMR  $\delta/ppm$ : 1.89 (6H, s, methyl), 2.00 (6H, s, methyl), 7.34-7.36 (6H, m, aromatic protons), 7.76-7.77 (4H, m, aromatic protons).  $^{13}C$  NMR  $\delta/ppm$ : 18.73 (methyl C), 25.28 (methyl C), 159.05, 163.54 (quaternary C's), 127.38, 128.67, 130.13, 134.69 (other C's). UV/VIS ( $C_2H_5OH$ )  $\lambda_{max}/nm$  ( $\epsilon/dm^3 mol^{-1} cm^{-1}$ ): 269 (33 100). ESI-MS  $m/z$ : 341.40 [(L+Na) $^+$ , 100%], 319.42 [(L+H) $^+$ , 70%].

#### 5.4 Synthesis of $[CuL_2]ClO_4$

Solid  $Cu(CH_3COO)_2 \cdot H_2O$  (0.100 g, 0.5 mmol) was added to a methanolic (25 ml) solution of L (0.318 g, 1 mmol). The resulting green reaction mixture was stirred for 2 h. To it  $NaClO_4$  (0.140g), dissolved in methanol (10 ml) was added and then left in air. An orange crystalline compound precipitated and was filtered off, washed with cold methanol (2 ml) and then dried in air. Yield, 0.23 g (55%). From this few orange crystals were selected for X-ray work. Anal. calcd for  $C_{40}H_{44}N_8CuClO_4$ : C, 60.07; H, 5.54; N, 14.01. Found: C, 60.29; H, 5.47; N, 13.93 %. FTIR  $\nu/cm^{-1}$ : 3433br, 2922w, 1614m, 1487w, 1443m, 1369m, 1248w, 1089vs, 939w, 775m, 746m, 694s, 669m, 623m, 569w.  $^1H$  NMR  $\delta/ppm$ : 2.00 (12H, s, methyl), 2.04 (12H, s, methyl), 7.38-7.41 (8H, m, aromatic protons), 7.46-7.49 (4H, m, aromatic protons), 7.62-7.64 (8H, m, aromatic protons).  $^{13}C$  NMR  $\delta/ppm$ : 20.64 (methyl), 26.81 (methyl C), 158.87, 168.24 (quaternary C's), 127.10, 129.41, 132.05, 133.12 (other C's). UV/VIS ( $C_2H_5OH$ )  $\lambda_{max}/nm$  ( $\epsilon/dm^3 mol^{-1} cm^{-1}$ ): 265 (50 900). ESI-MS  $m/z$ : 700.38 [( $CuL_2$ ) $^+$ , 65%].  $\Lambda_M/mho cm^2 mol^{-1}$ : 88 (1:1 electrolyte).

#### 5.5 Synthesis of $[CuL_2]PF_6$

Solid  $Cu(CH_3COO)_2 \cdot H_2O$  (0.100 g, 0.5 mmol) was added to a methanolic (25 ml) solution of 0.318 g (1 mmol) of L. The resulting green reaction mixture was stirred for 2 h. To it  $NH_4PF_6$  (0.190g) dissolved in methanol (10 ml) was added and then stirred for 1

h, a yellow precipitate was formed. It was filtered off, washed with cold methanol (2 ml) and then dried in air. Yield, 0.25 g (59%). Anal. calcd for  $C_{40}H_{44}N_8CuPF_6$ : C, 56.83; H, 5.25; N, 13.26. Found: C, 56.75; H, 5.29; N, 13.19 %. FTIR  $\nu/cm^{-1}$ : 3433br, 2922w, 1614m, 1445m, 1291w, 1250w, 1082w, 997w, 833vs, 777m, 748w, 694m, 667w, 559w.  $^1H$  NMR ( $CD_2Cl_2$ )  $\delta/ppm$ : 1.96 (12H, s, methyl), 2.05 (12H, s, methyl), 7.35-7.41 (8H, m, aromatic protons), 7.46-7.52 (4H, m, aromatic protons), 7.64-7.69 (8H, m, aromatic protons).  $^{13}C$  NMR ( $CD_2Cl_2$ )  $\delta/ppm$ : 20.64 (methyl C), 26.81 (methyl C), 158.87, 168.24 (quaternary C's), 127.10, 129.41, 132.05, 133.12 (other C's). UV/VIS ( $C_2H_5OH$ )  $\lambda_{max}/nm$  ( $\epsilon/dm^3 mol^{-1} cm^{-1}$ ): 265 (51 900). ESI-MS  $m/z$ : 700.38 [ $(CuL_2)^+$ , 65%].  $A_M/mho cm^2 mol^{-1}$ : 87 (1:1 electrolyte).

### 5.6 Synthesis of $[AgL_2]ClO_4$

$Ag(ClO_4).xH_2O$  (0.105 g, 0.5 mmol) dissolved in 5 ml of methanol was added drop wise to a methanolic (30 ml) solution of L (0.318 g, 1 mmol). The resulting pale yellow solution was stirred for 3 h and then left to evaporate slowly in the dark. When the volume reduced to ca 5 ml, the white crystalline compound precipitated and was filtered off, washed with cold methanol (2 ml) and then dried in air. Yield, 0.24 g (57%). Anal. calcd for  $C_{40}H_{44}N_8AgClO_4$ : C, 56.91; H, 5.25; N, 13.27. Found: C, 57.13; H, 5.16; N, 13.27 %. FTIR  $\nu/cm^{-1}$ : 3456br, 2916w, 1620s, 1568w, 1491w, 1444m, 1369s, 1244m, 1146w, 1115s, 1086vs, 926w, 777m, 694s, 625w, 569w.  $^1H$  NMR  $\delta/ppm$ : 2.00 (12H, s, methyl), 2.04 (12H, s, methyl), 7.37-7.41 (8H, m, aromatic protons), 7.45-7.49 (4H, m, aromatic protons), 7.62-7.64 (8H, m, aromatic protons).  $^{13}C$  NMR  $\delta/ppm$ : 20.41 (methyl C), 26.92 (methyl C), 159.19, 168.88 (quaternary C's), 127.04, 129.33, 132.05, 133.12 (other C's). UV/VIS ( $C_2H_5OH$ )  $\lambda_{max}/nm$  ( $\epsilon/dm^3 mol^{-1} cm^{-1}$ ): 273 (57 000). ESI-MS  $m/z$ : 744.28 [ $(AgL_2)^+$ , 100%].  $A_M/mho cm^2 mol^{-1}$ : 85 (1:1 electrolyte).

### 5.7 Synthesis of $[AgL_2]PF_6$

$AgNO_3$  (0.085 g, 0.5 mmol) dissolved in methanol (5 ml) was added dropwise to a methanolic (30 ml) solution of L (0.318 g, 1 mmol). The resulting pale yellow solution was stirred for 3 h and then  $NH_4PF_6$  (0.1 g) was added. After stirring the reaction mixture

for 1 h, it was left to evaporation air in the dark. When the volume reduced to ca 5 ml, a white crystalline compound precipitated which was filtered off, washed with cold methanol (2 ml) and then dried in air. Yield, 0.27 g (61%). Anal. calcd for  $C_{40}H_{44}N_8AgPF_6$ : C, 54.00; H, 4.98; N, 12.60. Found: C, 54.12; H, 5.10; N, 12.58 %. FTIR  $\nu/cm^{-1}$ : 3446br, 2920w, 1620s, 1444w, 1371m, 1246w, 1178w, 1076w, 833vs, 775m, 694s, 559s.  $^1H$  NMR  $\delta/ppm$ : 2.02 (12H, s, methyl), 2.10 (12H, s, methyl), 7.37-7.41 (8H, m, aromatic protons), 7.45-7.49 (4H, m, aromatic protons), 7.62-7.64 (8H, m, aromatic protons).  $^{13}C$  NMR  $\delta/ppm$ : 20.41 (methyl C), 26.92 (methyl C), 159.19, 168.88 (quaternary C's), 127.04, 129.33, 132.05, 133.12 (other C's). UV/VIS ( $C_2H_5OH$ )  $\lambda_{max} / nm$  ( $\epsilon / dm^3 mol^{-1} cm^{-1}$ ): 270 (58 900). ESI-MS  $m/z$ : 744.28  $[(AgL_2)^+, 100\%]$ .  $\Lambda_M/mho cm^2 mol^{-1}$ : 89 (1:1 electrolyte).

### 5.8 Incorporation of the compounds in PMMA

PMMA (80 mg) was dissolved in 1 ml of chloroform. 3 mmol of each compound studied was dissolved in this colourless solution.. The resulting yellow solution was thinly and evenly spread over a glass slide and dried in air to obtain a transparent film. The film, picked up by a sharp blade, was cut and shaped to a rectangle (1.2 cm x 5 cm). The thickness of the films was around 0.005 cm.

*Caution!* Care should be taken in handling perchlorates as they are potentially explosive. These should not be prepared and stored in large amounts.

### 5.9 X-ray structure determination

Single crystals were mounted on glass fibres and diffraction data collected on a Bruker AXS SMART APEX CCD diffractometer using Mo- $K\alpha$  radiation ( $\lambda = 0.71073 \text{ \AA}$ ). Data collection, indexing and initial cell refinements were all done using SMART [66] software. Data reduction was done with SAINT [67] software and the SADABS programme [68] was used to apply empirical absorption corrections. The structures were solved by direct methods [69] and refined by full matrix least-squares [70]. All non-hydrogen atoms were refined anisotropically and hydrogen atoms were included using a

riding model. Scattering factors were taken from International Tables for X-ray Crystallography [71]. Additional details of data collection and structure refinement are given in Table 1.

### **Acknowledgements**

S.G.P. thanks the Council of Scientific and Industrial Research, Government of India, New Delhi for a fellowship. Various help received from Dr. N. K. Shee are gratefully acknowledged.

### **Supplementary material available**

CCDC 1532964-1532966 contains the supplementary crystallographic data for L,  $[\text{CuL}_2]\text{ClO}_4$  and  $[\text{AgL}_2]\text{ClO}_4$ . These data can be obtained free of charge from the Cambridge Crystallographic Data Centre via [www.ccdc.cam.ac.uk/data\\_request/cif](http://www.ccdc.cam.ac.uk/data_request/cif). The  $^1\text{H}$  NMR spectra of L and  $[\text{CuL}_2]\text{ClO}_4$  in  $\text{CDCl}_3$  are given in the supplementary material as Figs. S1 and S2 respectively. The calculated NMR spectra are given in Table S1.

## References

- [1] W.-Y. Wong, C.-L. Ho, *Coord. Chem. Rev.* 253 (2009) 1709–1758.
- [2] Z.-Q. Chen, Z.-Q. Bian, C.-H. Huang, *Adv. Mater.* 22 (2010) 1534–1539.
- [3] Q. Zhao, F. Li, C. Huang, *Chem. Soc. Rev.* 39 (2010) 3007–3030.
- [4] L. Xiao, Z. Chen, B. Qu, J. Luo, S. Kong, Q. Gong, J. Kido, *Adv. Mater.* 23 (2011) 926–952.
- [5] H. Sasabe, J. Kido, *Chem. Mater.* 23 (2011) 621–630.
- [6] M.A. Baldo, D.F. O'Brien, Y. You, A. Shoustikov, S. Sibley, M.E. Thompson, S.R. Forrest, *Nature* 395 (1998) 151–154.
- [7] V. Marin, E. Holder, R. Hoogenboom, U.S. Schubert, *Chem. Soc. Rev.* 36 (2007) 618–635.
- [8] H. Yersin, A.F. Rausch, R. Czerwieniec, T. Hofbeck, T. Fischer, *Coord. Chem. Rev.* 255 (2011) 2622–2652.
- [9] R.D. Costa, E. Orti, H.J. Bolink, F. Monti, G. Accorsi, N. Armaroli, *Angew. Chem., Int. Ed.* 51 (2012) 8178–8211.
- [10] H. Xu, R. Chen, Q. Sun, W. Lai, Q. Su, W. Huang, X. Liu, *Chem. Soc. Rev.* 43 (2014) 3259–3302.
- [11] R. Visbal, M.C. Gimeno, *Chem. Soc. Rev.* 43 (2014) 3551–3574.
- [12] J. Chen, T. Teng, L. Kang, X.-L. Chen, X.-Y. Wu, R. Yu, C.-Z. Lu, *Inorg. Chem.* 55 (2016) 9528–9536.
- [13] P. Alam, C. Climent, G. Kaur, D. Casanova, A.R. Choudhury, A. Gupta, P. Alemany, I.R. Laskar, *Cryst. Growth Des.* 16 (2016) 5738–5752.
- [14] C. Ulbricht, B. Beyer, C. Friebe, A. Winter, U.S. Schubert, *Adv. Mater.* 21 (2009) 4418–4441.
- [15] K.-Y. Zhao, G.-G. Shan, Q. Fu, *Organometallics* 35 (2016) 3996–4001
- [16] A. Barbieri, G. Accorsi, N. Armaroli, *Chem. Commun.* 19 (2008) 2185–2193.
- [17] C.-W. Hsu, C.-C Lin, M.-W. Chung, Y. Chi, G.-H. Lee, P.-T. Chou, C.-H. Chang, P.-Y. Chen, *J. Am. Chem. Soc.* 133 (2011) 12085–12099.
- [18] M. Osawa, I. Kawata, R. Ishii, S. Igawa, M. Hashimoto, M.J. Hoshino, *Mater. Chem. C* 1 (2013) 4375–4383.

- [19] F. Dumur, *Org. Electron.* 21 (2015) 27–39.
- [20] C. Cho, H. Kang, S.-W. Baek, T. Kim, C. Lee, B.J. Kim, J.-Y. Lee, *ACS Appl. Mater. Interfaces* 8 (2016) 27911–27919.
- [21] K. Matsumoto, T. Shindo, N. Mukasa, T. Tsukuda, T. Tsubomura, *Inorg. Chem.* 49 (2010) 805–814,
- [22] D.G. Cuttell, S.-M. Kuang, P.E. Fanwick, D.R. McMillin, R.A. Walton, *J. Am. Chem. Soc.* 124 (2002) 6–7.
- [23] S.-M. Kuang, D.G. Cuttell, D.R. McMillin, P.E. Fanwick, R.A. Walton, *Inorg. Chem.* 41 (2002) 3313–3322.
- [24] A. Kaeser, B. Delavaux-Nicot, C. Duhayon, Y. Coppel, J.F. Nierengarten, *Inorg. Chem.* 52 (2013) 14343–14354.
- [25] S. Sculfort, P. Braunstein, *Chem. Soc. Rev.* 40 (2011) 2741–2760.
- [26] C.-M. Che, S.-W. Lai, *Coord. Chem. Rev.* 249 (2005) 1296–1309.
- [27] J.A Halfen, S. Mahapatra, E.C. Wilkinson, S. Kaderli, V.G. Young Jr., W.B. Tolman, *Science* 271 (1996) 1397–1400.
- [28] I. Garcia-Bosch, R.E. Cowley, D.E. Díaz, M.A. Siegler, W. Nam, E.I. Solomon, K.D. Karlin, *Chem. Eur. J.* 22 (2016) 5133–5137.
- [29] E.I. Solomon, *Inorg. Chem.* 55 (2016) 6364–6375.
- [30] S. Chowdhury, G.K. Patra, M.G.B. Drew, N. Chattopadhyay, D. Datta, *J. Chem. Soc., Dalton Trans.* (2000) 235–237.
- [31] S. De, D. Datta, *Int. J. Chem. Model.* 2 (2009) 7–14.
- [32] S. De, S. Chowdhury, D.A. Tocher, D. Datta, *CrystEngComm* 8 (2006) 670–673.
- [33] S. De, S. Chowdhury, J.P. Naskar, M.G.B. Drew, R. Clérac, D. Datta, *Eur. J. Inorg. Chem.* (2007) 3695–3700.
- [34] M. Abrahamsson, L. Hammarström, D.A. Tocher, S. Nag, D. Datta, *Inorg. Chem.* 45 (2006) 9580–9586.
- [35] G.A. Bowmaker, Effendy, S. Marfuaah, B.W. Skelton, A.H. White, *Inorg. Chim. Acta* 358 (2005) 4371–4388.
- [36] A.G. Young, L.R. Hanton, *Coord. Chem. Rev.* 252 (2008) 1346–1386.
- [37] A. Santoro, C. Sambigiagio, P.C. McGowan, M.A. Halcrow, *Dalton Trans.* 44 (2015) 1060–1069.

- [38] S. Chowdhury, M.G.B. Drew, D. Datta, *New J. Chem.* 27 (2003) 831–835.
- [39] M.T. Miller, P.K. Gantzel, T.B. Karpishin, *Angew. Chem., Int. Ed.* 37 (1998) 1556–1558.
- [40] S. Chowdhury, G.K. Patra, M.G.B. Drew, N. Chattopadhyay, D. Datta, *J. Chem. Soc., Dalton Trans.* (2000) 235–237
- [41] G. Raspi, L. Nucci, *Electroanal. Chem. Interfac. Chem.* 22 (1969) 139–146.
- [42] A. Grzejdzia, *Russ. Electrochem.* 29 (1993) 460–467.
- [43] D. Datta, H. A. O. Hill and H. Nakayama, *J. Electroanal. Chem.* 297 (1991) 309–314
- [44] D. Datta, H.A.O. Hill, H. Nakayama, *J. Electroanal. Chem.* 324 (1992) 307–323
- [45] R.F. Chen, *Anal. Lett.* 1 (1967) 35–42.
- [46] M.T. Buckner, D.R. McMillin, *J. Chem. Soc., Chem. Commun.* (1978) 759–761.
- [47] M.W. Blaskie, D.R. McMillin, *Inorg. Chem.* 19 (1980) 3519–3522.
- [48] C.T. Cunningham, J.J. Moore, K.L.H. Cunningham, P.E. Fanwick, D.R. McMillin, *Inorg. Chem.* 39 (2000) 3638–3644.
- [49] M. Iwamura, H. Watanabe, K. Ishii, S. Takeuchi, T. Tahara, *J. Am. Chem. Soc.* 133 (2011) 7728–7736.
- [50] M.K. Eggleston, D.R. McMillin, K.S. Koenig, A.J. Pallenberg, *Inorg. Chem.* 36 (1997) 172–176.
- [51] L.X. Chen, G.B. Shaw, I. Novozhilova, T. Liu, G. Jennings, K. Attenkofer, G.J. Meyer, P. Coppens, *J. Am. Chem. Soc.* 125 (2003) 7022–7034.
- [52] C.W. Hsu, C.C. Lin, M.W. Chung, Y. Chi, G.H. Lee, P.T. Chou, C.H. Chang, P.Y. Chen, *J. Am. Chem. Soc.* 133 (2011) 12085–12099.
- [53] R.M. Everly, D.R. McMillin, *Photochem. Photobiol.* 50 (1989) 711–716.
- [54] M.G.B. Drew, T.R. Pearson, B.P. Murphy, S.M. Nelson, *Polyhedron* 2 (1983) 269–274.
- [55] J.F. Dobson, B.F. Green, P.C. Healy, C.H.L. Kennard, C. Pakawatchai, A.H. White, *Aust. J. Chem.* 37 (1984) 649–659.
- [56] P. Purkayastha, N. Chattopadhyay, G.K. Patra, D. Datta, *Indian J. Chem.* 39A (2000) 375–377.

- [57] G.K. Patra, S. Samajdar, D. Datta, J. Chem. Soc., Dalton Trans. (2000) 1555–1558.
- [58] Gaussian 09, Revision C.01, M.J. Frisch, G.W. Trucks, H.B. Schlegel, G.E. Scuseria, M.A. Robb, J.R. Cheeseman, G. Scalmani, V. Barone, B. Mennucci, G.A. Petersson, H. Nakatsuji, M. Caricato, X. Li, H.P. Hratchian, A.F. Izmaylov, J. Bloino, G. Zheng, J.L. Sonnenberg, M. Hada, M. Ehara, K. Toyota, R. Fukuda, J. Hasegawa, M. Ishida, T. Nakajima, Y. Honda, O. Kitao, H. Nakai, T. Vreven, J.A. Montgomery, Jr., J.E. Peralta, F. Ogliaro, M. Bearpark, J.J. Heyd, E. Brothers, K.N. Kudin, V.N. Staroverov, T. Keith, R. Kobayashi, J. Normand, K. Raghavachari, A. Rendell, J.C. Burant, S.S. Iyengar, J. Tomasi, M. Cossi, N. Rega, J.M. Millam, M. Klene, J.E. Knox, J.B. Cross, V. Bakken, C. Adamo, J. Jaramillo, R. Gomperts, R.E. Stratmann, O. Yazyev, A.J. Austin, R. Cammi, C. Pomelli, J.W. Ochterski, R.L. Martin, K. Morokuma, V.G. Zakrzewski, G.A. Voth, P. Salvador, J.J. Dannenberg, S. Dapprich, A.D. Daniels, O. Farkas, J.B. Foresman, J.V. Ortiz, J. Cioslowski, D.J. Fox, Gaussian, Inc., Wallingford CT, 2010.
- [59] A.D. Becke, Phys. Rev. A 38 (1988) 3098–3100.
- [60] J.P. Perdew, Phys. Rev. B 33 (1986) 8800–8802.
- [61] J.P. Perdew, Phys. Rev. B 33 (1986) 8822–8824.
- [62] P.J. Hay, W.R. Wadt, J. Chem. Phys. 82 (1985) 270–283.
- [63] P.J. Hay and W.R. Wadt, J. Chem. Phys. 82 (1985) 299–310.
- [64] K.K. Baldridge, J.S. Siegel, J. Phys. Chem. A 103 (1999) 4038–4042.
- [65] P. Hemmerich, C. Sigwart, Experientia 19 (1963) 488–489.
- [66] *SMART* Version 5.628; Bruker AXS, Inc.: Madison, WI (2003).
- [67] *SAINTE* Version 6.36; Bruker AXS, Inc.: Madison, WI (2002).
- [68] Sheldrick, G. *SADABS* Version 2.10; University of Göttingen (2003).
- [69] Program XS from SHELXTL package, V. 6.12, Bruker AXS, Inc.: Madison, WI (2001).
- [70] Program XL from SHELXTL package, V. 6.12, Bruker AXS, Inc.: Madison, WI (2001).

- [71] A.J.C. Wilson, Ed. *International Tables for X-ray Crystallography, Volume C*; Kynoch, Academic Publishers: Dordrecht, 1992; Tables 6.1.1.4 (pp 500-502) and 4.2.6.8 (pp 219-222).

**Table 1**Selected crystallographic data for L, [CuL<sub>2</sub>]ClO<sub>4</sub> and [AgL<sub>2</sub>]ClO<sub>4</sub>

	L	[CuL <sub>2</sub> ]ClO <sub>4</sub>	[AgL <sub>2</sub> ]ClO <sub>4</sub>
Formula	C <sub>20</sub> H <sub>22</sub> N <sub>4</sub>	C <sub>40</sub> H <sub>44</sub> ClCuN <sub>8</sub> O <sub>4</sub>	C <sub>40</sub> H <sub>44</sub> ClAgN <sub>8</sub> O <sub>4</sub>
<i>M</i>	318.42	799.82	844.15
Temperature (K)	293(2)	293(2)	150(2)
Crystal System	monoclinic	monoclinic	orthorhombic
Space group	P2 <sub>1</sub> /n	C2/c	P2 <sub>1</sub> 2 <sub>1</sub> 2 <sub>1</sub>
Cell dimensions (Å, °)			
<i>a</i>	8.3224(6)	22.2164(15)	15.7595(9)
<i>b</i>	18.6230(13)	22.1042(15)	15.7934(9)
<i>c</i>	11.8431(8)	17.2452(12)	16.0104(9)
<i>α</i>	90.00	90.00	90.00
<i>β</i>	95.2700(10)	113.8660(10)	90.00
<i>γ</i>	90.00	90.00	90.00
<i>U</i> (Å <sup>3</sup> )	1827.8(2)	7744.6(9)	3984.9(4)
<i>Z</i> , <i>d</i> <sub>calc</sub> (g cm <sup>-3</sup> )	4, 1.157	8, 1.372	4, 1.407
<i>μ</i> (mm <sup>-1</sup> )	0.070	0.685	0.624
<i>F</i> (000)	680	3344	1744
Unique reflections	4351	9157	9544
Observed reflections [ <i>I</i> > 2σ( <i>I</i> )]	3295	8212	9030
<i>R</i> <sub>int</sub>	0.0229	0.0252	0.0195
Parameters	217	488	499
<i>R</i> <sub>1</sub> , <i>wR</i> <sub>2</sub> [ <i>I</i> > 2σ( <i>I</i> )]	0.0748, 0.2097	0.0496, 0.1225	0.0344, 0.0878
<i>R</i> <sub>1</sub> , <i>wR</i> <sub>2</sub> (all data)	0.0933, 0.2250	0.0554, 0.1261	0.0366, 0.0893
Largest peak/hole (e Å <sup>-3</sup> )	0.494/-0.154	0.656/-0.401	1.236/-0.500

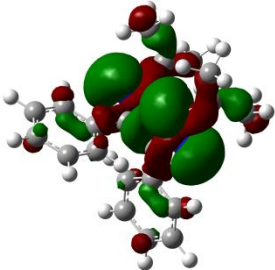
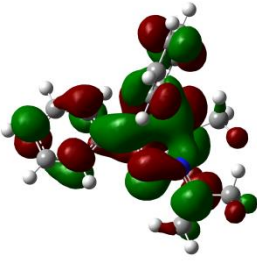
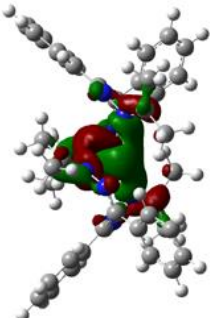
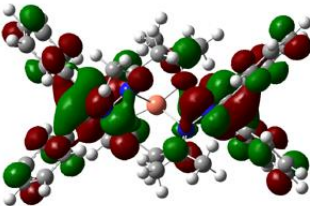
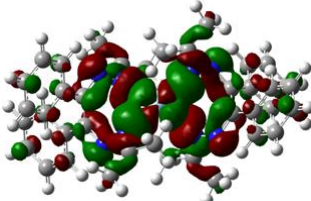
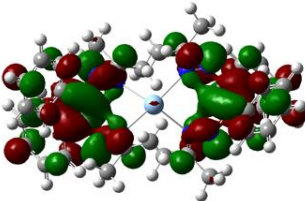
**Table 2**

Photoluminescence data for the metal complexes in deaerated ethanol at room temperature when excited at 270 nm

Species	$\lambda_{em}$ (nm)	$10^3 \times \phi$
[CuL <sub>2</sub> ]ClO <sub>4</sub>	400	0.97
[AgL <sub>2</sub> ]ClO <sub>4</sub>	387	0.69
[CuL <sub>2</sub> ] PF <sub>6</sub>	400	2.04
[AgL <sub>2</sub> ]PF <sub>6</sub>	388	3.37

**Table 3**

The HOMO's and LUMO's of various species, pertinent to the present work as obtained by DFT at the BP86/LanL2DZ level

species	HOMO	LUMO
L	 -4.809 eV	 -2.429 eV
[CuL <sub>2</sub> ] <sup>+</sup>	 -6.771 eV	 -5.154 eV
[AgL <sub>2</sub> ] <sup>+</sup>	 -7.421 eV	 -5.003 eV

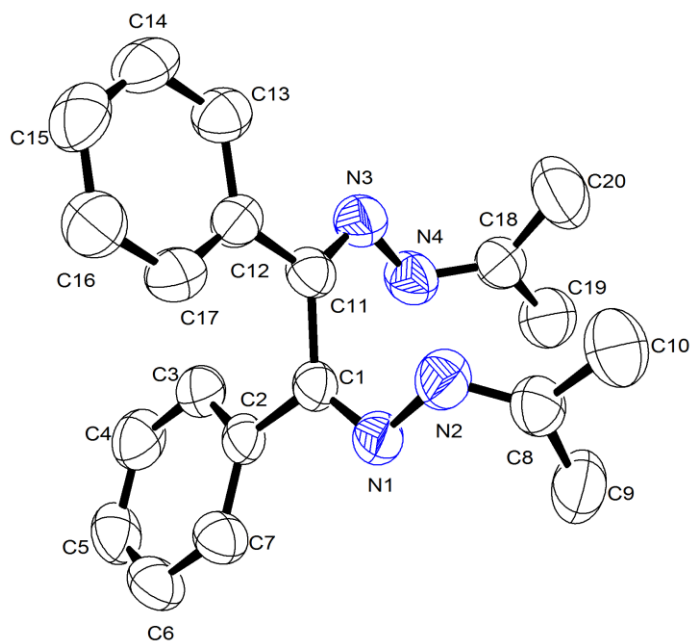


**Fig. 1** The molecular structure of L showing the atom numbering scheme (H atoms omitted for clarity and thermal ellipsoids at the 50% probability level). Selected bond lengths (Å) and bond angles (°): N(1)-N(2) 1.403(3), C(18)-C(20) 1.492(4), N(1)-C(1) 1.278(2), N(2)-C(8) 1.269(3), N(3)-N(4) 1.401(3), N(3)-C(11) 1.279(2), N(4)-C(18) 1.264(3), C(1)-C(11) 1.512(3), C(8)-C(9) 1.478(4), C(8)-C(10) 1.499(4), N(2)-N(1)-C(1) 114.44(17), C(12)-C(17)-C(16) 121.5(2), N(1)-N(2)-C(8) 114.79(19), N(4)-C(18)-C(19) 116.7(2), N4-N3-C11 113.12(17), N4-C18-C20 124.8(2), N3-N4-C18 117.28(19), C(19)-C(18)-C(20) 118.6(2), N(1)-C(1)-C(2) 118.81(17), N(1)-C(1)-C(11) 123.54(17).

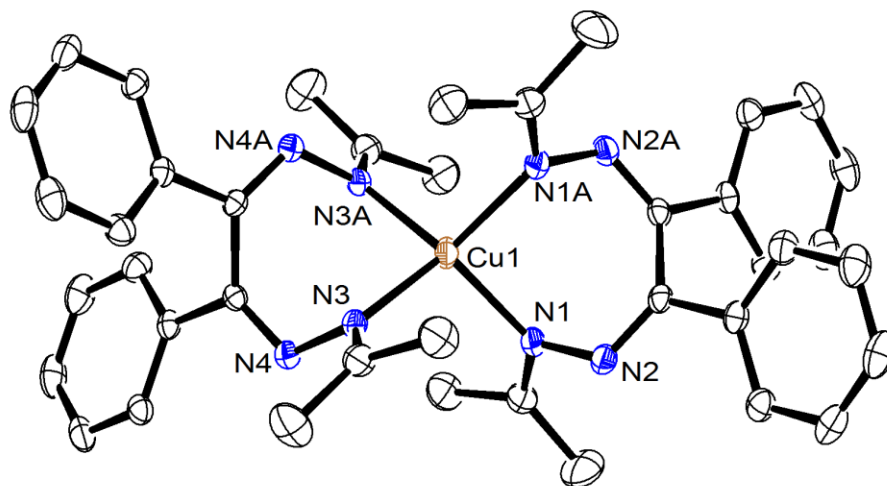


**Fig. 2** The molecular structure of one of the crystallographically unique cations in  $[\text{CuL}_2]\text{ClO}_4$  showing the atom numbering scheme (H atoms omitted for clarity and thermal ellipsoids at the 50% probability level). Selected bond lengths ( $\text{\AA}$ ) and bond angles ( $^\circ$ ): Cu(1)–N(1A) 2.0492(17), Cu(1)–N(1) 2.0492(17), Cu(1)–N(3) 2.0555(17), Cu(1)–N(3A) 2.0555(17), N(1A)–Cu(1)–N(1) 96.81(9), N(1A)–Cu(1)–N(3) 128.76(7), N(1)–Cu(1)–N(3) 105.34(7), N(1A)–Cu(1)–N(3A) 105.34(7), N(1)–Cu(1)–N(3A) 128.76(7), N(3)–Cu(1)–N(3A) 95.75(9).

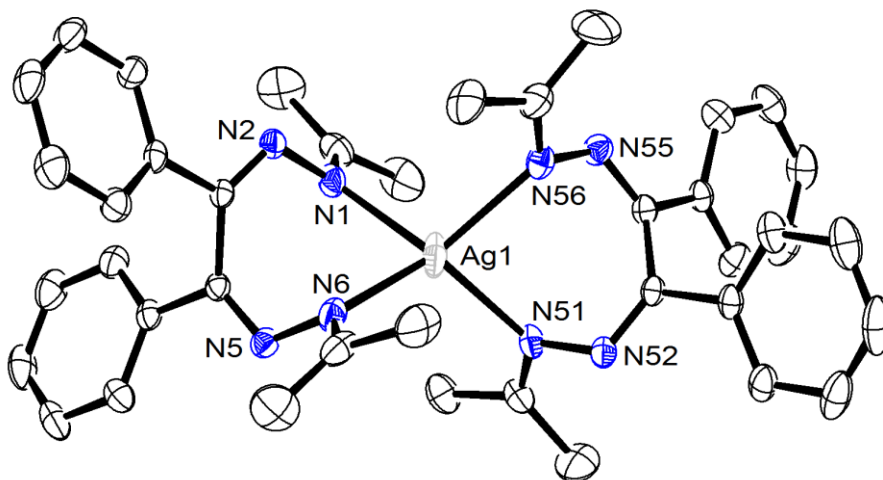


**Fig. 3** The molecular structure of the cation in  $[\text{AgL}_2]\text{ClO}_4$  showing the atom numbering scheme (H atoms omitted for clarity and thermal ellipsoids at the 50% probability level). Selected bond lengths ( $\text{\AA}$ ) and bond angles ( $^\circ$ ):  $\text{Ag}(1)\text{-N}(51)$  2.3014(19),  $\text{Ag}(1)\text{-N}(6)$  2.312(2),  $\text{Ag}(1)\text{-N}(56)$  2.3238(19),  $\text{Ag}(1)\text{-N}(1)$  2.330(2).  $\text{N}(51)\text{-Ag}(1)\text{-N}(6)$  117.54(7),  $\text{N}(51)\text{-Ag}(1)\text{-N}(56)$  89.12(6),  $\text{N}(6)\text{-Ag}(1)\text{-N}(56)$  128.96(7),  $\text{N}(51)\text{-Ag}(1)\text{-N}(1)$  129.30(7),  $\text{N}(6)\text{-Ag}(1)\text{-N}(1)$  88.86(6),  $\text{N}(56)\text{-Ag}(1)\text{-N}(1)$  107.47(7).

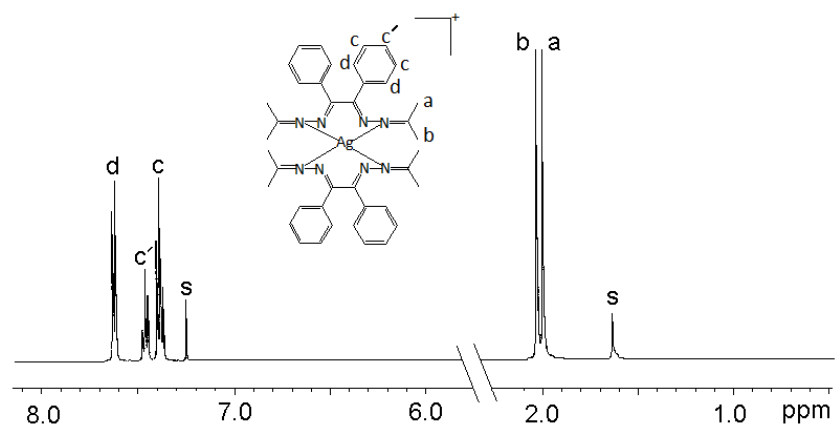


**Fig. 4** 500 MHz <sup>1</sup>H NMR spectrum of [AgL<sub>2</sub>]<sup>+</sup>ClO<sub>4</sub><sup>-</sup> in CDCl<sub>3</sub> indicating possible assignments (see also Table S1). Peaks marked by S are due to the solvent.

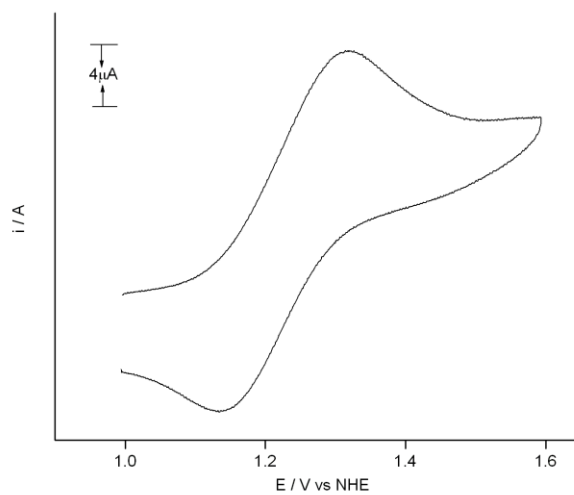


**Fig. 5** A portion of the cyclic voltammogram of  $[\text{CuL}_2]\text{ClO}_4$  in  $\text{CH}_2\text{Cl}_2$   $0.1 \text{ mol dm}^{-3}$  in tetrabutylammonium perchlorate (TBAP) under dry  $\text{N}_2$  atmosphere at a Pt electrode showing the Cu(II/I) couple. Solute concentration:  $1.01 \text{ mM}$ ; scan rate:  $100 \text{ mV s}^{-1}$ .

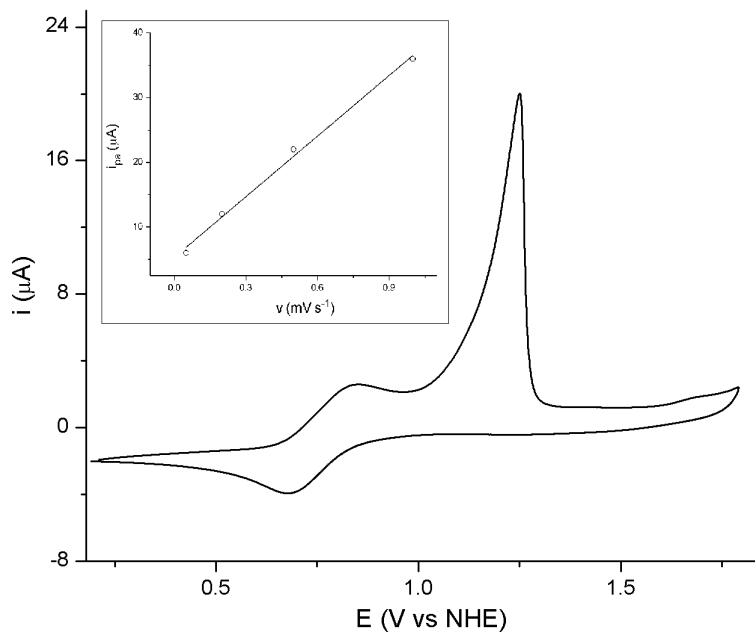


**Fig. 6** A portion of the cyclic voltammogram of [AgL<sub>2</sub>]ClO<sub>4</sub> in CH<sub>2</sub>Cl<sub>2</sub> 0.1 mol dm<sup>-3</sup> in tetrabutylammonium perchlorate (TBAP) under dry N<sub>2</sub> atmosphere at a Pt electrode showing the Ag(II/I) couple. Solute concentration: 1.01 mM; scan rate: 100 mV s<sup>-1</sup>. The inset shows the variation of anodic peak current *i*<sub>pa</sub> with scan rate *v* for the first electron transfer step (*r*<sup>2</sup> = 0.993).

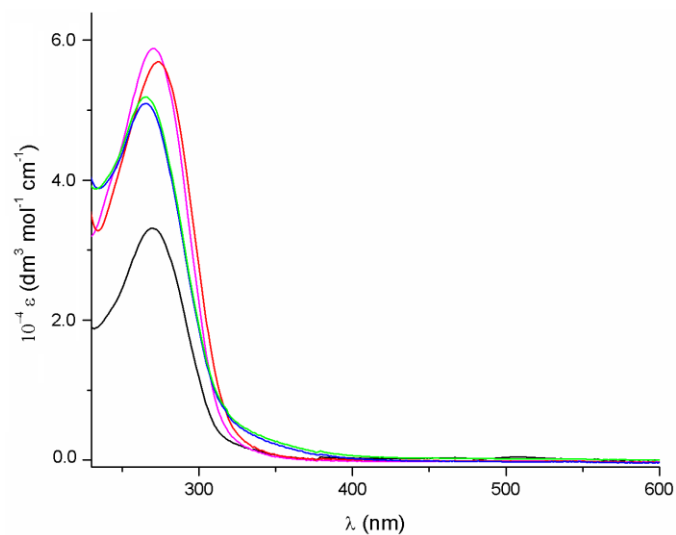


**Fig. 7** Absorption spectra of L (black trace), [CuL<sub>2</sub>]ClO<sub>4</sub> (blue trace), [CuL<sub>2</sub>]PF<sub>6</sub> (green trace), [AgL<sub>2</sub>]ClO<sub>4</sub> (red trace) [AgL<sub>2</sub>]PF<sub>6</sub> (magenta trace) in CH<sub>2</sub>Cl<sub>2</sub>. Concentration in each case was 1 x 10<sup>-5</sup> mol dm<sup>-3</sup>.

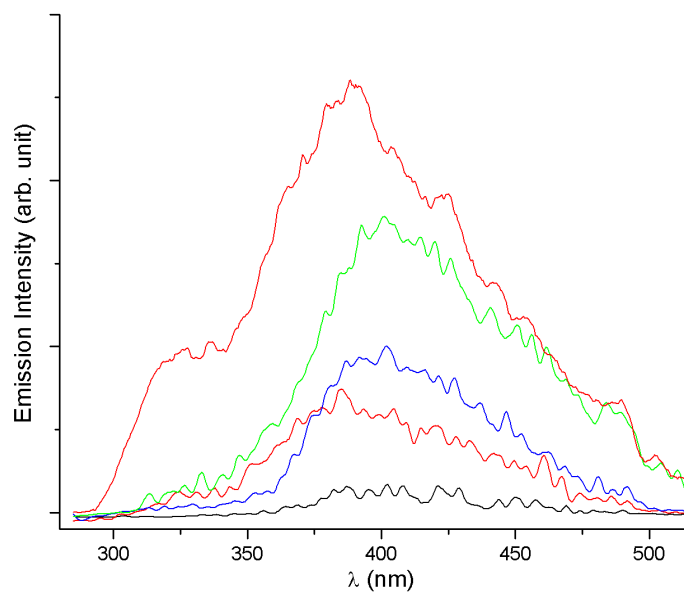


**Fig. 8** Emission spectra of L (black trace), [CuL<sub>2</sub>]ClO<sub>4</sub> (blue trace), [CuL<sub>2</sub>]PF<sub>6</sub> (green trace), [AgL<sub>2</sub>]ClO<sub>4</sub> (red trace) and [AgL<sub>2</sub>]PF<sub>6</sub> (pink trace) in deaerated ethanol. Excitation wavelength, 270 nm. Absorbance of each solution at 270 nm is 0.3.

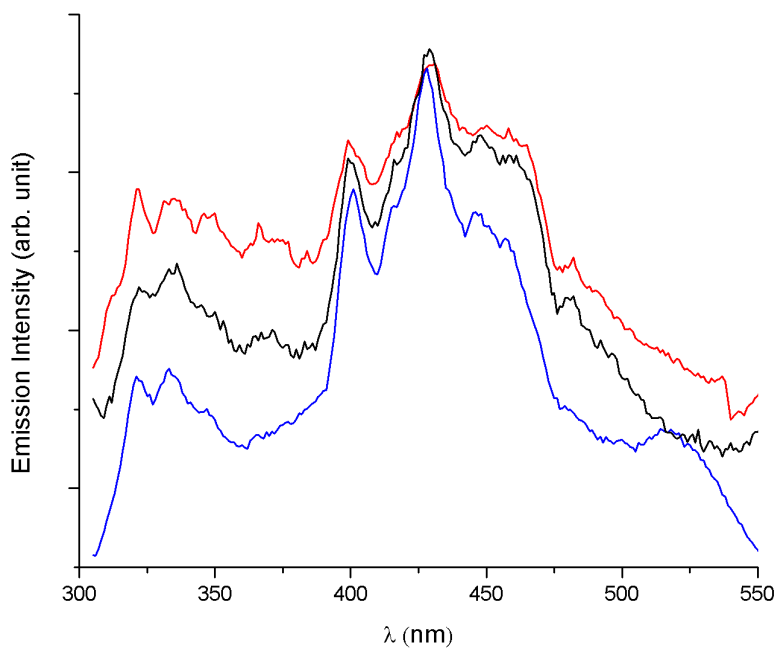


**Fig. 9** Emission spectra of L (black trace),  $[\text{CuL}_2]\text{ClO}_4$  (blue trace) and  $[\text{AgL}_2]\text{ClO}_4$  (red trace) in deaerated ethanol at 77 K. Excitation wavelength, 290 nm. Absorbance of each solution at 290 nm is 0.25.

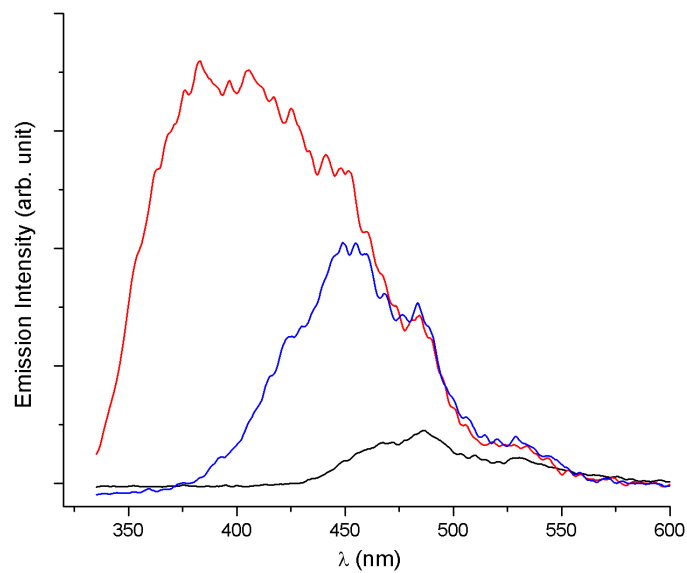


**Fig. 10** Emission spectra of L (black trace),  $[\text{CuL}_2]\text{ClO}_4$  (blue trace) and  $[\text{AgL}_2]\text{ClO}_4$  (red trace) in PMMA matrix. Excitation wavelength, 320 nm.